

On-orbit calibration of soft X-ray detector on Chang'E-2 satellite

Hong Xiao^a, Wenxi Peng^{a*}, Huanyu Wang^a, Xingzhu Cui^a, Dongya Guo^a

^aInstitute of High Energy Physics, CAS, Beijing, China

*Corresponding author at Institute of High Energy Physics, CAS, Beijing, China

Abstract—X-ray spectrometer is one of the satellite payloads on Chang'E-2 satellite. The soft X-ray detector is one of the device on X-ray spectrometer which is designed to detect the major rock-forming elements within 0.5-10keV range on lunar surface. In this paper, energy linearity and energy resolution calibration is done using a weak Fe⁵⁵ source, while temperature and time effect is considered not take big error. The total uncertainty is estimated to be within 5% after correction.

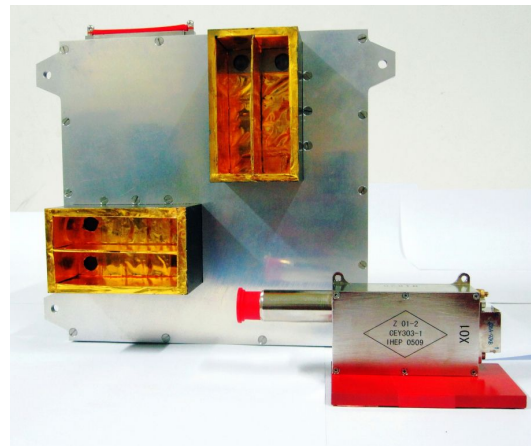
Keywords:SXD, calibration, on-orbit

1.Introduction

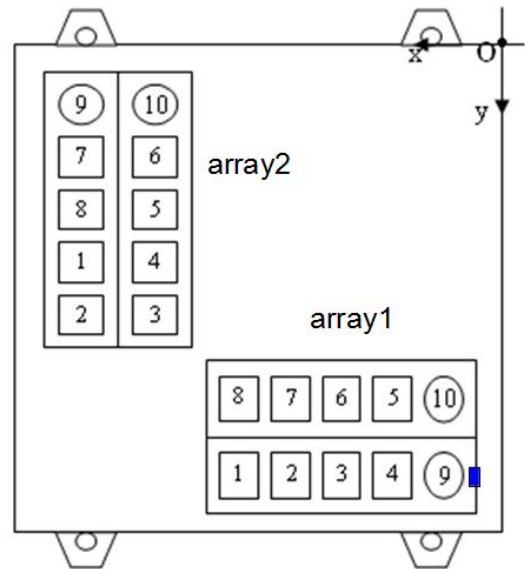
Following the precursor Chang'E-1(CE-1) satellite, a second lunar spacecraft of China, Chang'E-2 (CE-2), was launched on October 1, 2010. The CE-2 spacecraft resembled CE-1 mission with similar but the instrument performances were improved. With the onboard instruments, a huge amount of lunar scientific data were obtained successfully in CE-2 mission.

X-ray spectrometer (XRS) is one of the scientific payloads on CE-2. The XRS is composed of lunar X-ray detector (LXD) and solar X-ray monitor (SXM) which is shown in Fig.1A. The SXM is mainly used to monitor the solar X-ray flux and energy spectrum. LXD (the layout is shown in Fig.1B) is comprised of two perpendicular arrays. Each array includes two soft x-ray detectors which is used to detect the fluorescent X-rays within 1-10keV on lunar surface and eight hard x-ray detectors which is used to detect X-ray on lunar surface within energy range 25-60keV. Si-PIN X-ray sensors are used in each detector unit which equipped with bias circuits, charge sensitive preamplifiers and main amplifier circuits, while each detector unit work independently from each other. In order to monitor the performance variation of SXD, a weak Fe⁵⁵ source (~1μCi) was glued inside the collimator close to the Be window which is also shown in Fig.1B. Table 1 shows the specification of the SXDs.[1]

The scientific goal of the XRS is to obtain the abundance distribution of the major rock-forming elements (Mg, Al, Si, Ca, Ti, Fe and etc.) on lunar surface. Precise results can be got by accumulating the data in each area of the lunar surface to have enough statistics, but before this energy calibration should be done first. Energy calibration generally includes calibration of energy linearity and energy resolution. The result of on-orbit calibration using Fe⁵⁵ source will be introduced in this article.[2]



A)



B)

Fig. 1A. X-ray spectrometer on CE-2(left: lunar x-ray detector; right: Solar X-ray monitor)
1B. X-ray spectrometer structure(circle is SXD, rectangle is HXD, blue rectangle is Fe⁵⁵ source)

Table1: the performance of SXD

components	Soft detector(SXD)	X-ray
objects	Lunar fluorescence	X-ray
detector	Si-PIN*4 chips	
filter	12.5 μ m beryllium	
energy range	0.5-10 keV	
effective area	1cm ²	
energy resolution	300 eV@5.9 keV	
ADC	10 bits	

2.on-orbit calibration of Energy linearity and resolution calibration

CE-2 satellite goes into circumlunar orbit from October 2nd, 2010. The data of X-ray spectrometer is transferred to the ground-based system from October 15th, 2010. About 7 months' data was obtained for this analysis, which include the message of longitude, latitude, height, quality state and etc. In this section, we select the events in good quality for the on-orbit calibration analysis from Oct. 18th, 2010 to Oct. 20th, 2010 which solar flare level higher than C5(solar flares higher than $5 \times 10^{-6} \text{W/m}^2$ between 1 and 8 angstroms detected by NOAA satellites).[3]

X-ray will lose energy in the sensitive medium of the detector. The detection of incident photon energy is actually the detection of photon energy lose in the detector. For the X-ray photons which deposit all the energies in the detector, the channel of electronic signal represents the incident X-ray energy. So that the relation between energy and channel can directly obtained, then channel-count spectrum can be converted into energy-count spectrum. In a word, the principle of energy linearity calibration is calibrating the correlation between different X-ray energy and the channel of electronic signal.

Mean ionization energy of semiconductor has no relationship with incident X-ray energy, so electronic signal which detector produced keep linear with incident X-ray energy.

Linear fit is used in calibration for energy-channel curve, the fitting equation is

$$E = K \times ch + \Delta E$$

Where Ch is channel, E is incident X-ray energy, K is slope, ΔE is intercept.[4]

The full energy peaks of Ca, Mn and Fe are fitted with gaussian to do the energy linearity and resolution calibration. The fitting result of one detector is shown in Fig.2. Four soft X-ray detectors are calibrated independently. The detailed fit result is shown in Table 2.

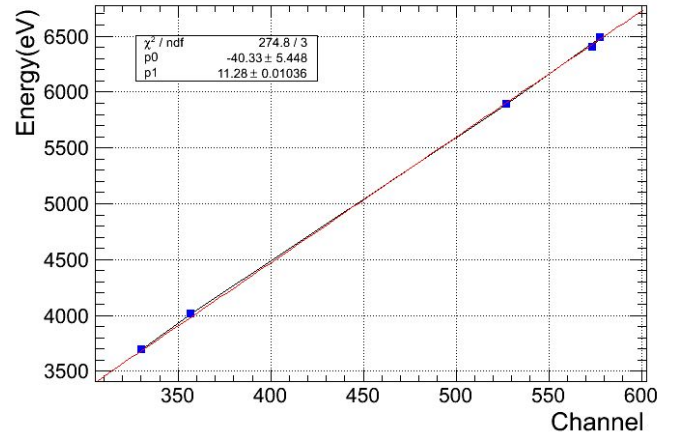


Fig. 2. The plot is the energy linearity calibration plot which shows the correlation between channel and energy.

Energy resolution of the detector is usually evaluated with FWHM of the full energy peak. The full energy spectrum of Monoenergetic X-ray in X-ray spectrometer is gaussian spectrum from theoretical estimation and calibration experiment analysis. So the energy spectrum of Si-PIN detector can be fit with gaussian distribution.

Energy resolution of X-ray spectrometer can be influenced by two factors. One is statistic fluctuation of random process in ionization, the other is caused by the noise generated by the electronic system.

The first factor is relevant to incident X-ray energy(ΔE_1), the relationship can be described with the function: $\Delta E_1 = (kE)^{1/2}$

The second factor has nothing to do with incident X-ray energy (ΔE_2). According to the error propagation equation, FWHM can be expressed as:

$$FWHM = \sqrt{\Delta E_1^2 + \Delta E_2^2} = \sqrt{KE + \Delta E^2}$$

Function 3 is used in fitting energy resolution curve.

Fig. 3 is the fitting result of energy resolution calibration which shows the correlation between energy and FWHM.

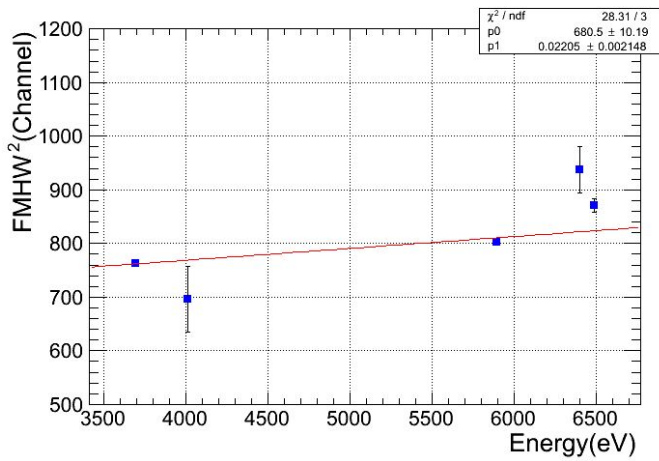


Fig. 3. The energy resolution calibration result plot.

3.on-orbit calibration using radioactive sources and calibration uncertainties

Because of the different environment in space, calibration result will be different. There are two factors affecting the on-orbit performance of SXD: performance changes with the orbit for short-term; space radiation damage caused by long-term degradation.

The main mechanisms of space radiation damage silicon detectors are total dose effects and displacement effects. Both effects will cause dark current increasing, the energy resolution decreasing. On circumlunar orbit, space radiation is mainly from the galactic cosmic rays, solar energetic particles and high energy electrons.

Through on-orbit calibration data with weak Fe^{55} radioactive source (only affect SXD array1-9), orbit-variation and time-variation of SXD performance are analyzed in this section.

Due to there are active temperature control systems, Signal fluctuation of the Soft X-ray detector almost not affect by the outside temperature, but the electronic noise increases as the temperature increases. The energy resolution of the detector will deteriorate while temperature increases.

There are three thermal sensors (TMR130, TMR146 and TMR147) on X-ray spectrometer, which can detect the temperature of the solar X-ray monitor, lunar x-ray detector and electronic crate respectively. However, the temperature of TMR146 is the temperature of the X-ray spectrometer shell, there is an unknown temperature gradient in the vacuum environment, so it's not the exact temperature of the temperature sensitive device. Except that the parameter

of the detector post-amplifier will change while time changes. So the temperature of TMR146 is just taken as reference.

Because CE-2 is a polar orbit satellite, the orbital period is about 127 minutes, there are no big change in longitude in every cycle(only about 1°), then we find there is a positive relation between the temperature of TMR146 and the latitude, about 6 hours' comparison on Oct 20th,2010 was shown in Fig. 4 for example. We select the data in a fixed latitude range, and then divide the data into several longitude bins will see the change.[5]

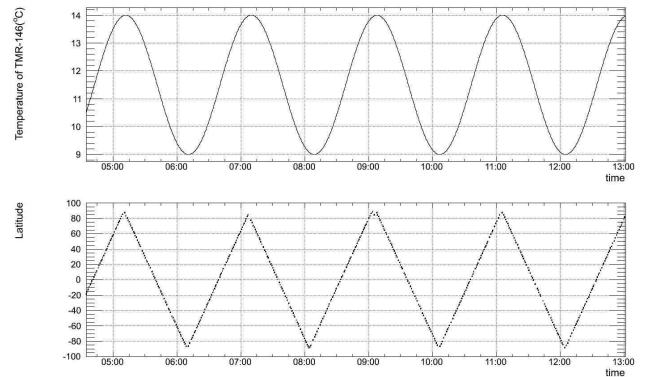
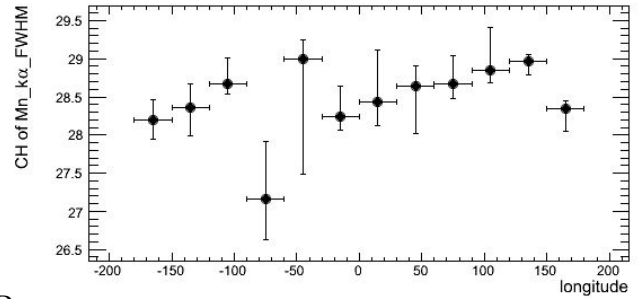
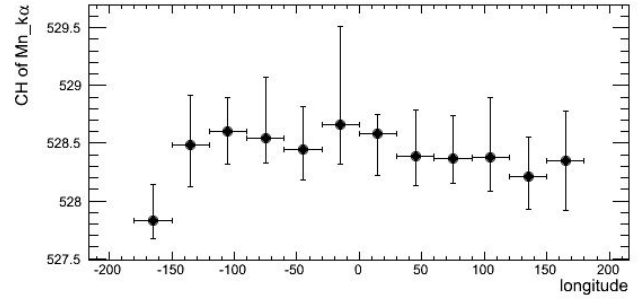
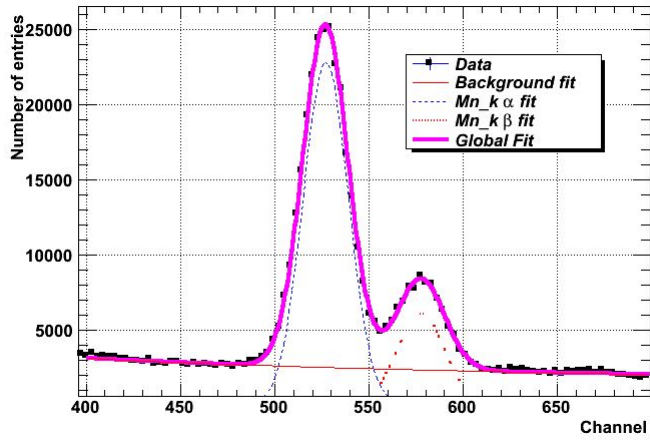


Fig. 4. The relationship between temperature and latitude on Oct 20th, 2010(top: Temperature of TMR-146 vs. time bottom: latitude vs. Time)

Powerful solar flare will affect the calibration result, so we first select the data which solar flare level lower than C5. Because temperature is related to longitude and latitude, $30^\circ \times 30^\circ$ small grids(longitude 12bins, latitude 6 bins) are taken to be analyzed so as to eliminate the temperature effect, which can be thought temperature almost do not change in every grid. Time effect is first checked, Mn peak in every single grid in every month is separately fitted as in Fig.5A. The relation between calibration and time is detailedly shown in Fig.5B, there are six months' data is in the every individual plot, every point is the result of one month data fit, we can see no fixed regular tendency in the figure. Because of the different environment, the average energy resolution (about 28 channels) on-orbit became a little larger than ground-based result (about 26 channels) as we expected. Then latitude is fixed in range 60° to 90° to see the calibration change while the longitude changes in Fig. 5C, every point upper limit means the maximum value in 6 months in the longitude bin, while lower limit means the minimum value, and the point position is the fit result of the whole 6 months. Longitude is also fixed in range 0° to 30° to see the calibration change while the latitude changes in Fig. 5D. The detailed result of the peak position in each grid of one month is shown in Table3-4.



A B
C D

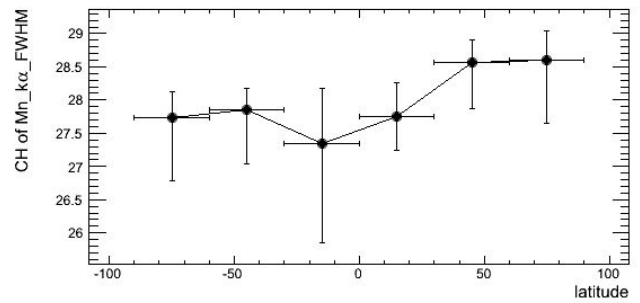
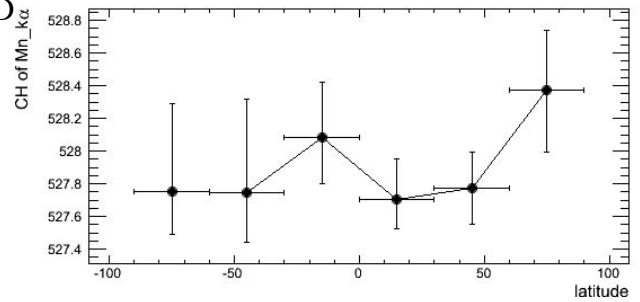
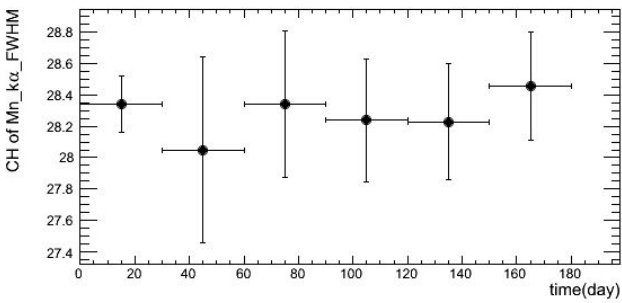
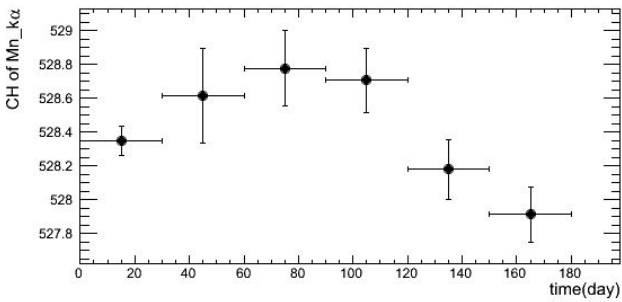


Fig. 5A. Fe⁵⁵ full energy peak fit example in one of the 30°×30° grid for one month

Fig. 5B. Calibration result change with time (top: peak position, bottom: FWHM unit: channel)

Fig. 5C. Calibration result change with longitude while latitude range within 60° to 90° (top: peak position, bottom: FWHM, unit: channel)

Fig. 5D. Calibration result change with latitude while longitude range within 0° to 30° (top: peak position, bottom: FWHM, unit: channel)

We suppose that peak position and FMHW calibration result in every month in every grid almost not affected by time, in order to get the element distribution on lunar surface, full energy peak position should be corrected with the parameters so as not to take in extra uncertainty. The efficiency detection result is supposed to take very small uncertainty. Then the systematic error of the FMHW in every grid is thought to be taken by time effect, the total error is shown in Fig. 6, which including both statistical error and systematic error, the element distribution error in the grid can be estimated by this figure. We can get the conclusion that the global calibration is within 5% during the mission.

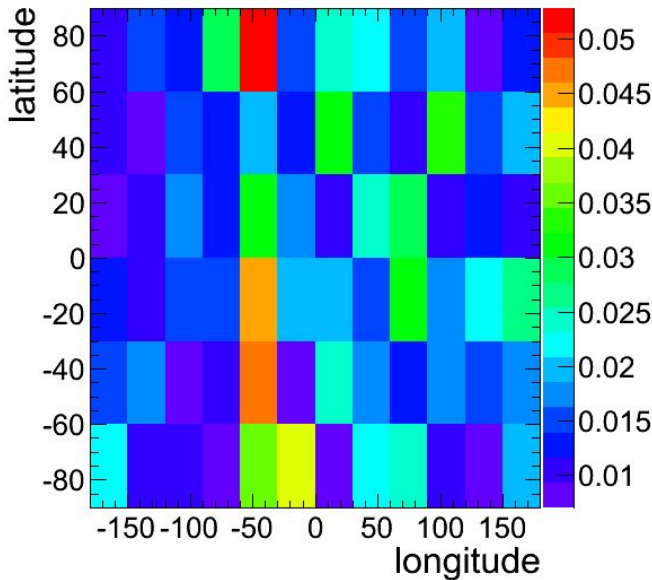


Fig. 6: energy peak and resolution vs. Latitude(left:the first month data right: the last month data)

Table 2: on-orbit calibration of energy peak and energy resolution

	E vs. Channel		FWHM vs. E	
	K	C	K	C
Array1-9	11.28	-49.80	0.0239	661.89
Array1-10	10.97	-22.86	0.0386	637.70
Array2-9	11.47	6.38	0.1384	171.82
Array2-10	10.52	-4.47	-0.0411	993.68

Table 3. First month Fe-55 peak position calibration result(unit: channel)

latitude \ longitude	-90°to-60°	-60°to-30°	-30°to0°	0°to30°	30°to60°	60°to90°
-180°to-150°	527.732 ± 0.086	527.766 ± 0.085	528.008 ± 0.087	527.383 ± 0.082	527.495 ± 0.085	527.830 ± 0.090

4. Conclusion

In order to satisfy the scientific goal of the CE-2 project, calibrations of soft X-ray detector are well designed and successfully accomplished. On-orbit calibration are used to check the performance of each soft X-ray detectors. Energy linearity and energy resolution are calibrated using Fe⁵⁵ source. The temperature and time effect is also taken account of, while no big shift is found. The overall calibration uncertainty is estimated to be within 5%.

5. Acknowledgment

We thank the National Astronomical Observatories of the Chinese Academy of Sciences (NAOC) for providing the on-orbit data. We also extremely thank the reviewers for improving the paper.

REFERENCES

- [1] Peng Wen-Xi, et.al. Chinese Physics C, 819(2009)33
- [2] ZUO Wei, et.al. Chin.J.Geochem.(2014)33:024-044
- [3] <http://spaceweather.com/glossary/flareclasses.html>
- [4] M. Grande, et.al. Planetary and Space Science 57(2009)717 - 724
- [5] Stefanie L. Lawson, et.al. JOURNAL OF GEOPHYSICAL RESEARCH, VOL. 105, NO. E2, PAGES 4273-4290, FEBRUARY 25, 2000

-150°to-120°	527.749±0.086	527.879±0.084	527.748±0.081	527.616±0.082	527.868±0.084	528.486±0.087
-120°to-90°	528.184±0.078	528.012±0.078	527.967±0.085	528.020±0.080	528.430±0.088	528.607±0.089
-90°to-60°	528.289±0.082	528.207±0.087	528.200±0.087	528.080±0.090	528.592±0.091	528.539±0.095
-60°to -30°	528.047±0.103	527.952±0.108	527.665±0.108	527.555±0.107	528.384±0.114	528.446±0.115
-30° to 0°	527.848±0.106	527.946±0.106	527.894±0.102	528.134±0.101	528.294±0.101	528.660±0.099
0°to30°	528.164±0.093	527.997±0.088	528.418±0.087	528.168±0.088	528.286±0.087	528.582±0.094
30°to60°	527.867±0.088	528.220±0.086	527.690±0.088	527.742±0.088	528.277±0.090	528.391±0.091
60°to90°	527.775±0.083	527.784±0.083	528.081±0.084	527.690±0.086	527.745±0.084	528.365±0.090
90°to120°	527.901±0.085	527.718±0.089	527.594±0.092	527.652±0.089	527.882±0.088	528.381±0.086
120°to150°	527.752±0.085	527.801±0.082	527.628±0.084	528.204±0.083	527.731±0.082	528.207±0.084
150°to180°	527.828±0.084	527.912±0.082	527.694±0.082	527.971±0.085	527.983±0.084	528.350±0.086

Table 4. 6th month Fe-55 peak position calibration result(unit: channel)

latitude longitude	-90°to-60°	-60°to-30°	-30°to0°	0°to30°	30°to60°	60°to90°
-180°to-150°	527.361±0.169	527.503±0.161	527.826±0.167	527.122±0.157	527.297±0.163	527.672±0.174
-150°to-120°	527.608±0.171	527.748±0.169	527.574±0.161	527.495±0.163	527.885±0.166	528.119±0.174
-120°to-90°	527.990±0.152	527.932±0.152	527.736±0.162	527.813±0.158	528.144±0.165	528.316±0.168
-90°to-60°	528.251±0.160	528.143±0.169	528.075±0.168	527.971±0.175	528.311±0.170	528.331±0.179
-60°to -30°	527.970±0.191	527.778±0.195	527.551±0.198	527.564±0.198	528.156±0.206	528.205±0.212
-30° to 0°	527.593±0.199	527.852±0.198	527.723±0.196	527.927±0.194	528.120±0.193	528.316±0.191
0°to30°	527.795±0.171	527.944±0.166	528.288±0.166	528.143±0.169	528.173±0.163	528.527±0.173
30°to60°	527.728±0.167	528.062±0.163	527.560±0.165	527.858±0.167	528.187±0.166	528.195±0.167
60°to90°	527.559±0.157	527.642±0.158	527.952±0.158	527.654±0.161	527.696±0.156	528.233±0.167
90°to120°	527.621±0.159	527.416±0.168	527.370±0.173	527.469±0.167	527.621±0.167	528.087±0.165
120°to150°	527.568±0.157	527.435±0.151	527.488±0.155	528.010±0.152	527.592±0.152	528.041±0.158
150°to180°	527.471±0.157	527.746±0.155	527.552±0.153	527.892±0.157	527.807±0.157	527.914±0.165